ECCOMAS Congress 2016
VII European Congress on Computational Methods in Applied Sciences and Engineering
M. Papadrakakis, V. Papadopoulos, G. Stefanou, V. Plevris (eds.)
Crete Island, Greece, 5–10 June 2016

FORCED RESPONSE OF SHROUDED BLADES WITH VARIABLE OPERATING POINTS

Ferhat Kaptan[1], Lars Panning-von Scheidt[2], Jörg Wallaschek[3], Victor Salit[4]

[1,2,3]Institute of Dynamics and Vibration Research, Leibniz Universität Hannover
Appelstraße 11, 30167 Hannover, Germany
[1] kaptan@ids.uni-hannover.de
[2] panning@ids.uni-hannover.de
[3] wallaschek@ids.uni-hannover.de

[4]MAN Diesel & Turbo SE
Steinbrinkstraße 1, 46145 Oberhausen, Germany
[4] victor.salit@man.eu

Keywords: shrouded blades, nonlinear vibration, friction.

Abstract. *The variable operation of turbomachinery components turns out as a special challenge in the design process. Changing the turbines rotational speed leads to entirely new load conditions and, thus, to a range of different operating points. Beside structural mechanical dependencies (i.e. stiffening effects), the shroud contact situation is very sensitive to the systems rotational speed. In this paper a model of a real low pressure steam turbine blade is investigated numerically and experimentally. For the calculation, a three dimensional structural mechanical model including a spatial contact model is considered. The steady-state vibration response is calculated by the multi-harmonic balance method (MHBM) and an alternating frequency-time scheme (AFT). The test rig consists of a single blade clamped with two dummies at the shroud. The vibration response of the blade is measured by laser-doppler-vibrometry for various excitation levels and pressure distributions in the shroud contact. The comparison between measured and computed frequency response function (FRF) of the first edgewise bending mode (1E) shows a very good agreement. Both the frequency shift, as well as the reduction of the amplitude were detected by the MHBM and successfully verified experimentally. The obtained results of the single blade system are transferred to a rotating bladed disk assembly.*

1 INTRODUCTION

One of the main challenges in the mechanical design of turbine blades is the prevention of high cycle fatigue (HCF) failures. Successful blade design must account for both high static, caused for example by centrifugal forces, and high dynamic loads, caused, among others, by oscillating forces of the working fluid. These loads, even the static ones, depend on the turbines operating condition. However, not only the loading, but also material parameters, like the elastic modulus, and structural mechanical properties, like the damping ratio, and stiffening or softening of the blade, depend on the turbines operating condition. Indeed, material properties are temperature dependent, the tangent stiffness is stress dependent and the overall damping depends on many factors simultaneously - stress, temperature, contact pressure at the joints. Friction in the joints like the blade root or the blade tip shrouds can be used to dissipate the vibrational energy and, thus, the amplitude of the blade vibrations. However, the nonlinear dependence of the relative displacements on the contact pressure and thus on the operational condition, makes the design for friction a very challenging task.
Nonlinear steady-state forced response analysis, which can aid in such a design, has been a subject of active research for the last three decades [1–5]. However, a forced response analysis under variable operating conditions remained largely unstudied.
In this study, we analyze two different operating points with respect to the turbines rotational speed. The investigation is performed both experimentally and numerically. The experimental setup consists of a single model blade, fixed at its root, with variable contact pressure applied at the shroud through two dummies, mounted on air bearing. The blade is excited by shaker and the frequency response function (FRF) was measured using laser-doppler-vibrometry for various excitation and contact pressure levels. These results were used to verify the numerical approach, based on the multi-harmonic balance method (MHBM), described in [6] and [7], in which the nonlinear forces are computed by the means of an alternating frequency-time (AFT) scheme [8].

2 FORCED RESPONSE CALCULATION

2.1 Computation of the steady state solution by the multi-harmonic balance method

The dynamical behavior of a nonlinear mechanical system can be described by the following equation of motion in the time domain:

$$\mathbf{M}\ddot{\mathbf{u}}(t) + \mathbf{D}\dot{\mathbf{u}}(t) + \mathbf{K}\mathbf{u}(t) + \mathbf{f}_{\text{nl}}(\dot{\mathbf{u}}(t), \mathbf{u}(t)) = \mathbf{f}_{\text{e}}(t) \tag{1}$$

where $\mathbf{M}$, $\mathbf{D}$, $\mathbf{K}$ are the mass, viscous damping and stiffness matrices. The external force is denoted by $\mathbf{f}_{\text{e}}$ and the nonlinear force by $\mathbf{f}_{\text{nl}}$. For a forced response analysis, the external force $\mathbf{f}_{\text{e}}$ is assumed to be a harmonic function

$$\mathbf{f}_{\text{e}}(t) = \Re\left\{\hat{\mathbf{f}}_{\text{e}}\text{e}^{\text{i}\Omega t}\right\}. \tag{2}$$

In the linear case, i.e. $\mathbf{f}_{\text{nl}} = 0$, the resulting displacements, $\mathbf{u}(t)$, are harmonic functions with frequency Ω. In the presence of nonlinearities, e.g. contact forces, the response function $\mathbf{u}(t)$ is no longer harmonic, but nevertheless assumed to be periodic. This assumption allows the approximation of the displacments' vector $\mathbf{u}$, as well as the nonlinear forces $\mathbf{f}_{\text{nl}}$, by a truncated Fourier series. This so-called multi-harmonic balance method (MHBM) is widely used to compute the nonlinear forces in conjunction with an alternating frequency-time scheme (AFT) [8].

Applying Galerkin's procedure the nonlinear equations of motion (1) can be rewritten in the frequency domain with the complex displacements

$$\mathbf{u}(t) = \Re\left\{\sum_{n=0}^{n_\mathrm{h}} \hat{\mathbf{u}}_n \mathrm{e}^{\mathrm{i}n\Omega t}\right\} \tag{3}$$

and the complex nonlinear forces

$$\mathbf{f}_\mathrm{nl}(t) = \Re\left\{\sum_{n=0}^{n_\mathrm{h}} \hat{\mathbf{f}}_{\mathrm{nl},n} \mathrm{e}^{\mathrm{i}n\Omega t}\right\} \tag{4}$$

as

$$\hat{\mathbf{S}}_n \hat{\mathbf{u}}_n + \hat{\mathbf{f}}_{\mathrm{nl},n} - \hat{\mathbf{f}}_{\mathrm{e},n} = \mathbf{R}_n. \tag{5}$$

Here, $\hat{\mathbf{S}}_n$ is the dynamic stiffness matrix

$$\hat{\mathbf{S}}_n = -(\Omega n)^2 \mathbf{M} + \mathrm{i}\Omega n \mathbf{D} + \mathbf{K} \tag{6}$$

and $\mathbf{R}_n$ denotes the residual vector. The set of nonlinear equations (5) constitutes a minimization problem, which has to be solved iterative by means of a Newton-Raphson algorithm. To reduce the computational effort, a model reduction of the dynamic system is performed by the well-known Craig-Bampton reduction technique [10].

2.2 Contact Model

In this study, an elastic point contact model is used to compute the nonlinear contact forces, see Fig. 1, a widely used model in dynamical systems with frictional contacts [6, 7, 11]. For the calculation of a three-dimensional spatial contact, it is assumed that the tangential components are independent of each other, a common assumption in forced response calculations with frictional contacts [7].

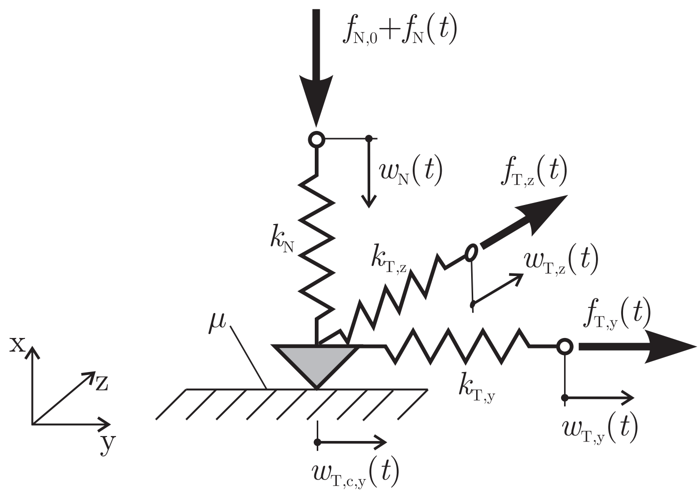

Figure 1: Unilateral elastic contact model

The normal force $f_\mathrm{N}(t)$ is given by the normal relative displacement $w_\mathrm{N}(t)$ and the contact stiffness k_N. The contact state ratio, closed or separated, depends on the static preload $f_{\mathrm{N},0}$ and determined by the unilateral contact law

$$f_{\mathrm{N}}(t) = \max\left(f_{\mathrm{N},0} + k_{\mathrm{N}} w_{\mathrm{N}}(t), 0\right). \tag{7}$$

A negative preload value of $f_{\mathrm{N},0}$ is equivalent to a gap between the contact nodes and is defined as $g_{\mathrm{N},0} = -f_{\mathrm{N},0}/k_{\mathrm{N}}$. The contact force along the tangential directions y and z is given by the contact stiffness $k_{\mathrm{T},j}$ and the tangential relative displacement $w_{\mathrm{T},j}(t)$, for $j = y, z$. The Coulomb friction law is applied to determine the state ratio in tangential direction by

$$f_{\mathrm{T}}(t) = \begin{cases} k_{\mathrm{T},j}(w_{\mathrm{T},j}(t) - w_{\mathrm{T,c},j}(t)) & \text{sticking contact,} \\ \mu f_{\mathrm{N}}(t)\mathrm{sgn}(w_{\mathrm{T,c},j}(t)) & \text{sliding contact,} \\ 0 & \text{separation.} \end{cases} \tag{8}$$

3 APPLICATION TO SHROUDED TURBINE BLADES

3.1 Mechanical model of a single turbine blade

A model of a single low pressure shrouded turbine blade is investigated, see Fig. 2a. For convenience, the root of the blade is modeled as a rectangular block and the angular pitch is set to zero. The neighbored blades are simplified as dummies with high masses mounted by frictionless supports, see Fig. 2b. Thus, the normal load on the shroud can be stated as $f_{\mathrm{N}} = f_{\mathrm{L}} \sin\alpha$. Compared to a fully assembled bladed disk, changing the loading f_{L} is representing a

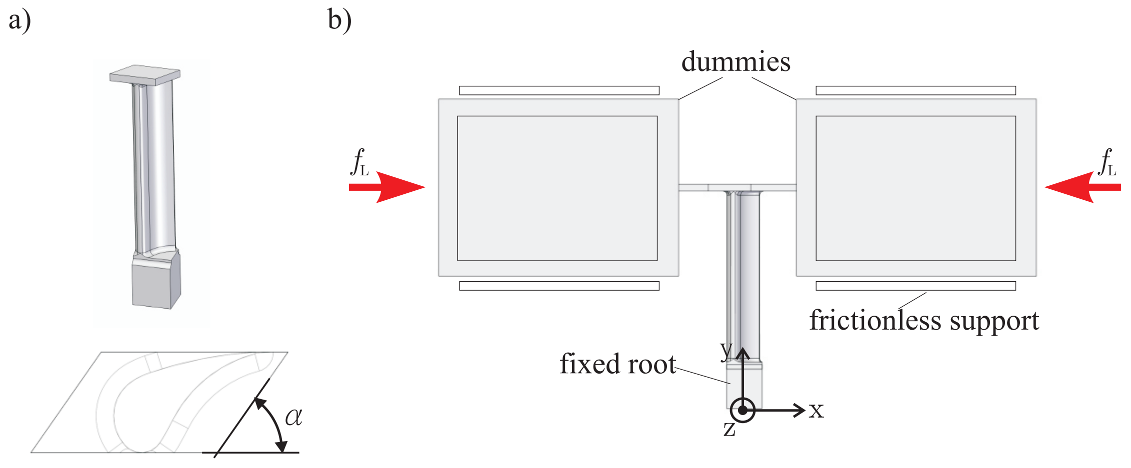

Figure 2: a) Single shrouded turbine blade, b) experimental setup.

variation of the turbine's operating point. Nevertheless, a change of the operating point of the real turbine influences in addition the pressure distribution at the shroud contact or the structural mechanical properties due to centrifugal stiffening. Since the main objective of the presented experimental setup is the correlation between excitation load f_{e}, preload f_{L} and the response of the system, here, the variation of the pressure distribution as the centrifugal stiffening is neglected.

Finite element analysis is used to discretize the shown model with a total number of 16755 elements and 28112 nodes. The shroud contact area is discretized with 30 contact nodes. The structural mechanical matrices $\mathbf{M}$ and $\mathbf{K}$ of the whole system read:

$$\mathbf{M} = \begin{bmatrix} \mathbf{M}_{\mathrm{Blade}} & \mathbf{0} & \mathbf{0} \\ \mathbf{0} & \mathbf{M}_{\mathrm{Dummy,L}} & \mathbf{0} \\ \mathbf{0} & \mathbf{0} & \mathbf{M}_{\mathrm{Dummy,R}} \end{bmatrix}, \mathbf{K} = \begin{bmatrix} \mathbf{K}_{\mathrm{Blade}} & \mathbf{0} & \mathbf{0} \\ \mathbf{0} & \mathbf{K}_{\mathrm{Dummy,L}} & \mathbf{0} \\ \mathbf{0} & \mathbf{0} & \mathbf{K}_{\mathrm{Dummy,R}}, \end{bmatrix}. \quad (9)$$

In the first instance, there are uncoupled submatrices in (9). The coupling of the substructures takes place in the nonlinear calculation by contact forces.
In this work the first flapwise bending mode (1F) and the first edgewise bending mode (1E) of the coupled system is investigated. The mode shapes of the coupled and the free standing blade are showed in Fig. 3. Note that the mode shapes are calculated assuming a rigid coupling of the linear system in the case of Fig. 3b. It should be emphasized here that a full separating of the contact is leading to a completely different dynamical system behavior. For the nonlinear forced response, contact parameters must be specified, i.e. contact stiffnesses, friction coefficient and pressure distribution. The contact stiffnesses are defined by a magnitude of 10^9 N/m and the friction coefficient is set for all simulations to $\mu = 0.3$. The pressure distribution is calculated by a quasi-static nonlinear FE-analysis.

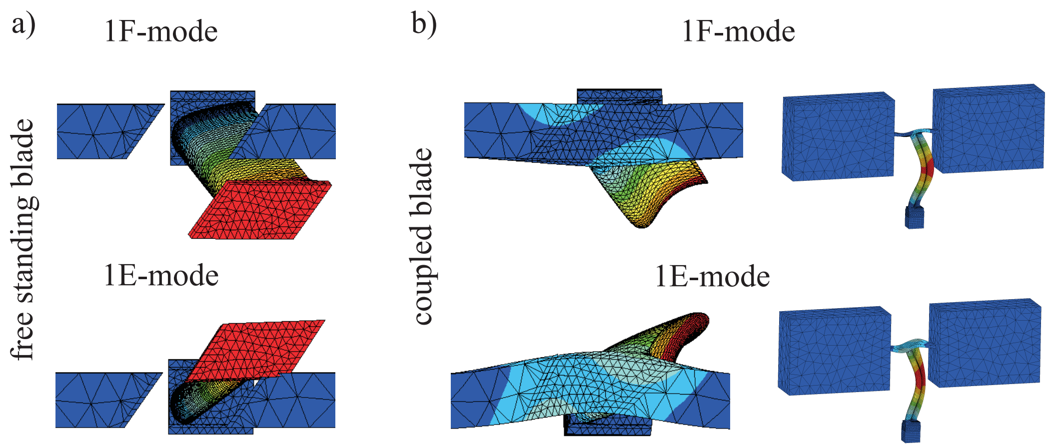

Figure 3: First two mode shapes of: a) the free standing, b) coupled blade.

3.2 Experimental Setup

The test rig in Fig. 4 is used to measure the forced response of the coupled structure. A shaker is set up for the force excitation and the vibration amplitudes are measured by laser-doppler-vibrometry. Due to the strong nonlinearities a controlled force amplitude is necessary. Hence, the excitation force is measured by a piezoelectric force sensor and controlled to the desired excitation level. Weights are applied by rope pulleys to impress the normal loading. The frequency response function is measured for various excitation levels and normal loadings. It is important to note that the measurements are based on the fundamental harmonic.

4 Results

4.1 Comparison of experiment and simulation

The experimental results show that the resonance frequencies of both modes are sensitive to a variation of the normal load f_{L}, see Fig. 5a and b. The reason for this effect depends on

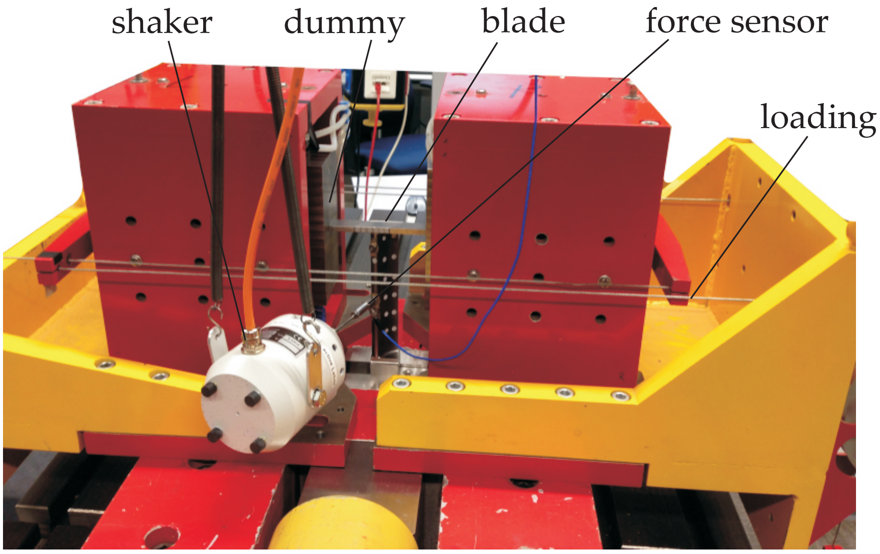

Figure 4: Test rig.

the mode shape and the contact kinematics. In Fig. 5b the maximum amplitude of the 1E-mode decreases for increasing excitation level f_e or decreasing normal load f_L, a well-known phenomenon of underplatform damper mechanics, see [9]. Due to high relative displacements in tangential direction of the shroud area sliding friction forces are leading to energy dissipation and, thus, to lower amplitudes. Besides, the resonance frequency significantly decrease due to microslip phenomena in the contact area. The 1F-mode shows a quiet different vibrational behavior. The mode shape depends highly on the contact situation and pressure distribution. Separation of the contact results to a shift of the nodal point of the mode shape and much higher amplitudes at the tip of the blade. Nevertheless, friction damping still occurs at the shroud area that is more dominant for lower normal loads, see Fig. 5a. A comparison to the simulation results shows a good agreement. The amplitudes are in the same order of magnitude and, in particular, a relative error of the resonance frequencies of $\frac{\Delta f}{f_0} < 1\%$ is remarkable. In addition, the amplitude reduction caused by friction of the 1E-mode correlates well to the experiment, see Fig. 5b. Note that the amplitude reduction depends on the friction coefficient, which is set to $\mu = 0.3$. The reduction of the resonance frequency due to microslip can also be shown by the simulation model. The simulation results of the 1F-mode show the same dynamical behavior as the experiment, see Fig. 5a. According to Eq. (7) either low normal preloads or high relative displacements lead to separation and at the same time to a loss of contact stiffness. Consequently the FRFs tend to tilt to the left side. However, the increase of the amplitude caused by a change of the mode shape can not be shown by the simulation model. This is motivated by the underlying Craig-Bampton reduction technique [10]. Here, the constraint interfaces are defined by the contact areas and, thus, the fixed interface modes are based on the coupled system.

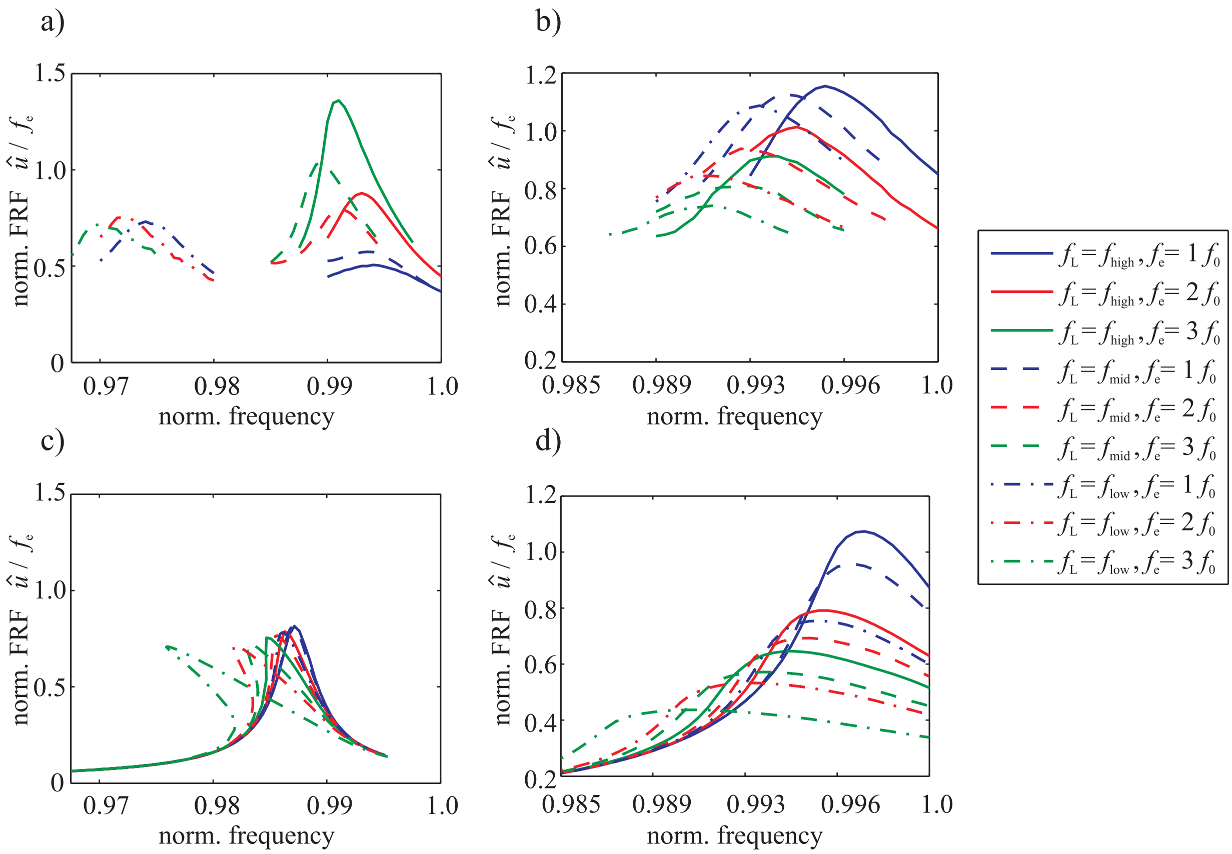

Figure 5: Forced response functions of the experiment a), b) and the simulation c), d) for various excitation levels and preloads.

4.2 Computation of a tuned bladed disk assembly

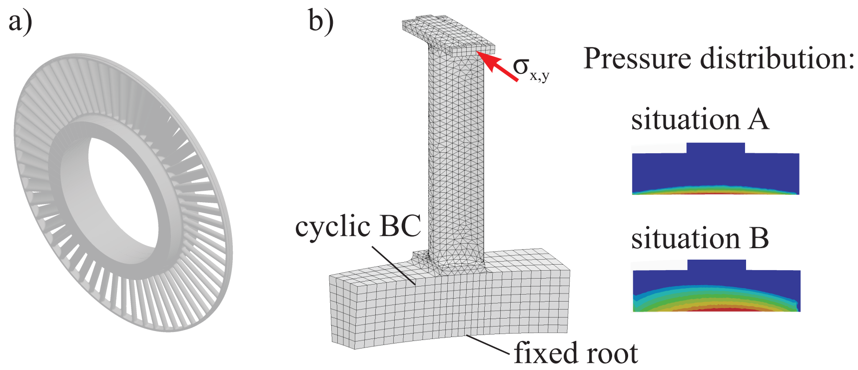

Figure 6: a) Bladed disk assembly, b) FE-model of a cyclic sector and calculated pressure distribution.

In this section a bladed disk with $N_{\text{Seg}} = 60$ blades is analyzed, see Fig. 6a. All blades are assumed to be perfectly tuned and, thus, cyclic symmetry can be used to reduce the computational effort. Two different operating points with respect to the pressure distribution at the shroud contact are investigated, see Fig. 6b. For the forced response analysis Eq. 1 is set up for one cyclic segment. The displacement vector for any segment k is

$$^{(k)}\mathbf{u}(t) = \mathrm{e}^{-\mathrm{i}(k-1)\Delta\varphi}\ {}^{(1)}\mathbf{u}(t) \tag{10}$$

where $k = 1(1)N_{\mathrm{Seg}}$ and $\Delta\varphi = 2\pi/N_{\mathrm{Seg}}$ denotes the phase angle [12].
The results of the bladed disk assembly show similar characteristics as the single blade system, see Fig. 7. For pressure distribution A only the lower edge of the shrouds is in contact and the total preload is concentrated on the edge. The FRFs of the 1F-mode show strong nonlinear characteristics, see Fig. 7a. Due to the high normal relative displacement the contact closes and the stiffness of the dynamical system increases strongly. Increasing the excitation force or decreasing the preload is leading to lower maximum amplitudes due to frictional energy dissipation. Changing the pressure distribution, the FRF of the 1F-mode seems to be strongly influenced, see Fig. 7b. Again, an increase of the excitation level leads to lower amplitudes and a shift of the frequency at maximum amplitude. But, at a low preload value local separation of the contact appears and the FRF is tending to lower frequencies. The occurrence of a closing and a separating contact at once have a high impact on the convergence behavior. Care must be taken when choosing numerical parameters. The 1E-mode of the cyclic system is rarely influenced by the variable pressure distribution, see Fig. 7b and d. Both cases show the same behavior as the single blade system in Fig. 5d. The slight increase of the resonance frequencies at pressure distribution B is caused by increased initial contact area and, thus, by higher stiffness.

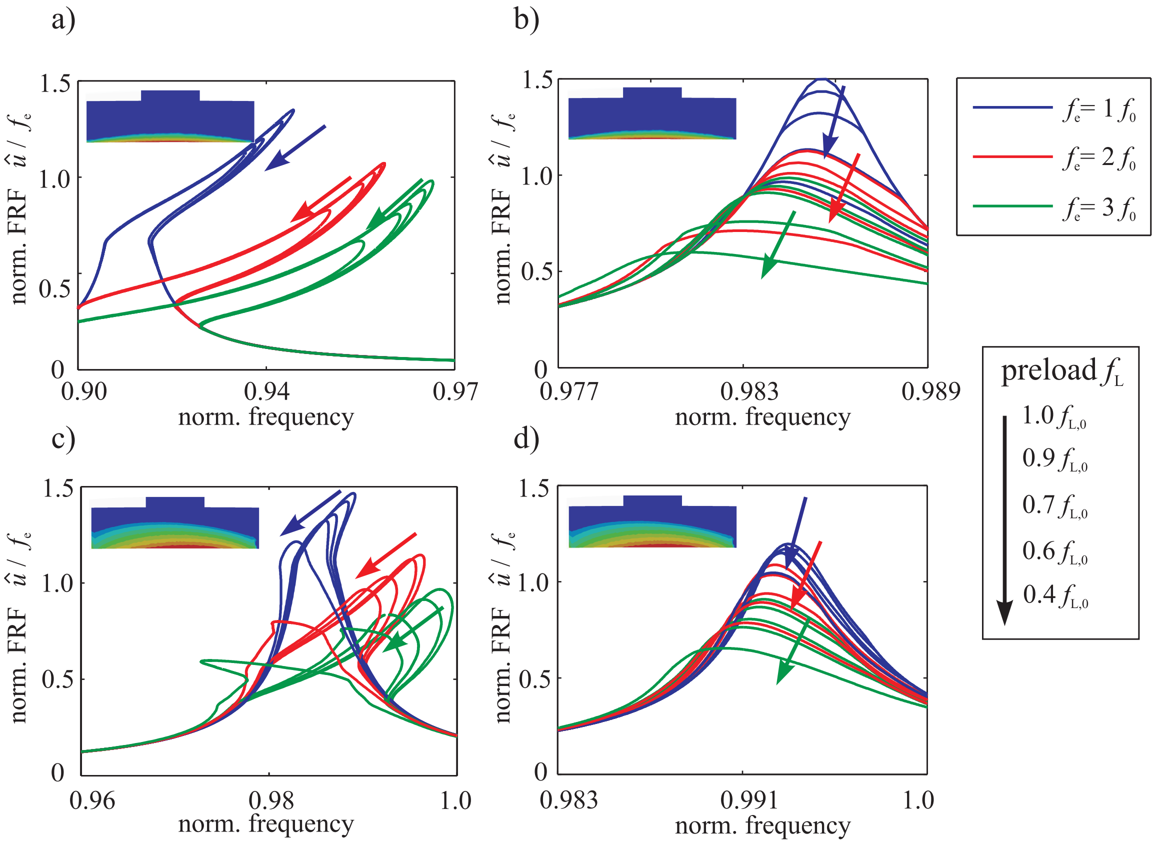

Figure 7: FRF of the 1F- and 1E-mode of the cyclic system (nodal diameter=25) for various preloads and excitation levels: a), b) pressure distribution A, c), d) pressure distribution B.

5 Conclusion and outlook

In this paper the dynamical behavior of a turbine blade model is analyzed numerically and experimentally. A comparison shows a very good agreement, qualitatively as well as quantitatively. The results are transferred to a rotating bladed disk. Two different operating points with respect to the pressure distribution are investigated showing similar phenomena as the single blade system. Regarding variable operating points turns out as a special challenge due to a high sensitivity by minor changes in the shroud contact. In particular, large relative displacements in normal direction may affect the convergence. The outlook of the work is the experimental investigation of a rotating bladed disk assembly for various operating points, i.e. rotational speed.

Acknowledgements. The investigations were conducted as part of the joint research programme COOREFlex-turbo in the frame of AG Turbo. The work was supported by the Bundesministerium für Wirtschaft und Technologie (BMWi) as per resolution of the German Federal Parliament under grant number 03ET7020K. The authors gratefully acknowledge AG Turbo and MAN Diesel & Turbo SE for their support and permission to publish this paper. The responsibility for the content lies solely with its authors.

REFERENCES

[1] Menq, C.-H., Griffin, J. H., Bielak, J.: *The forced response of shrouded fan stages.* Journal of Vibration and Acoustics 108.1: 50-55, 1986.

[2] Yang, B. D., Menq, C.-H.: *Modeling of friction contact and its application to the design of shroud contact.* Journal of Engineering for Gas Turbines and Power (Trans. ASME), Vol. 119, no. 4, pp. 958-963, 1997.

[3] Sextro, W.: *The calculation of the forced response of shrouded blades with friction contacts and its experimental verification.* ASME-Paper 2000-GT-540, Proceedings of the ASME Turbo Expo 2000, Munich (Germany), 2000.

[4] Szwedowicz, J., Sextro, W., Visser, R., Masserey, P. A.: *On forced vibration of shrouded turbine blades.* ASME-Paper GT2005-69062, Proceedings of the ASME Turbo Expo 2003, Atlanta (USA), 2003.

[5] Krack, M., Herzog, A., Panning-von Scheidt, L., Wallaschek, J., Siewert, C., and Hartung, A.: *Multiharmonic Analysis and Design of Shroud Friction Joints of Bladed Disks Subject to Microslip.* ASME 2012 International Design Engineering Technical Conferences and Computers and Information in Engineering Conference. American Society of Mechanical Engineers, 2012.

[6] Petrov, E. P., Ewins, D. J.: *Analytical Formulation of Friction Interface Elements for Analysis on Nonlinear Multi-Harmonic Vibrations of Bladed Discs Discs.* ASME-Paper GT-2002-30325, Proceedings of the ASME Turbo Expo 2002, Amsterdam, Netherlands, 2002.

[7] Siewert, C., Panning-von Scheidt, L., Wallaschek, J., Richter, C.: *Multiharmonic forced response analysis of a turbine blading coupled by nonlinear contact forces.* Paper GT2009-59201, Proc. of ASME Turbo Expo 2009: Power for Land, Sea and Air, GT2009, June 8-12, Orlando, Florida, USA, 2009.

[8] Cameron, T. M., Griffin, J. H.: *An Alternating Frequency/Time Domain Method for Calculating the Steady-State Response of Nonlinear Dynamic Systems.* Journal of Applied Mechanics, Vol. 56, pp. 149-154, 1989.

[9] Panning, L.: *Auslegung von Reibelementen zur Schwingungsdämpfung von Turbinenschaufeln.* Fortschrittberichte VDI, Reihe 11: Schwingungstechnik, Nr. 328,VDI-Verlag, Düsseldorf, 2005

[10] Craig, R. R., Bampton, M. C. C.: *Coupling of Substructures for Dynamic Analyses.* AIAA Journal, 6(7), pp. 13131319, 1968.

[11] Cigeroglu, E., An, N., Menq, C. H.: *A Microslip Friction Model with Normal Load Variation induced by Normal Motion.* Nonlinear Dynamics, Vol. 50(3), pp. 609-626, 2007.

[12] Thomas, D. L.: *Dynamics of Rotationally Periodic Structures.* International Journal for Numerical Methods in Engineering, Vol. 14, pp. 81-102, 1979.